Indian J Phys (December 2015) 89(12):1251–1263
DOI 10.1007/s12648-015-0696-6

ORIGINAL PAPER

Half-metallic ferromagnetism in $Be_{1-x}V_xTe$ alloys: an Ab-initio study

M El Amine Monir[1], R Khenata[1], G Murtaza[2]*, H Baltache[1], A Bouhemadou[3], Y Al-Douri[4,5], S Azam[6], S Bin Omran[7] and H Ud Din[8]

[1]Laboratoire de Physique Quantique et de la Modélisation Mathématique, Université de Mascara, 29000 Mascara, Algeria

[2]Materials Modeling Lab, Department of Physics, Islamia College University, Peshawar 25000, Pakistan

[3]Laboratory for Developing New Materials and their Characterization, Department of Physics, Faculty of Science, University Setif 1, 19000 Setif, Algeria

[4]Institute of Nano Electronic Engineering, University Malaysia Perlis, 01000 Kangar, Perlis, Malaysia

[5]Department of Physics, Faculty of Science, University of Sidi-Bel-Abbes, 22000 Sidi Bel Abbes, Algeria

[6]New Technologies - Research Center, University of West Bohemia, Univerzitni 8, 306 14 Pilsen, Czech Republic

[7]Department of Physics and Astronomy, College of Science, King Saud University, P.O. Box 2455, Riyadh 11451, Saudi Arabia

[8]Department of Physics, Hazara University, Mansehra 21110, Pakistan

Received: 17 January 2015 / Accepted: 26 March 2015 / Published online: 16 May 2015

Abstract: First-principles calculations of the structural, elastic, electronic, magnetic and thermodynamic properties of zinc blende $Be_{1-x}V_xTe$ alloys ($x = 0$, 0.25, 0.50, 0.75 and 1) based on spin-polarized density functional theory are performed using full-potential augmented plane wave method, within the spin generalized gradient approximation for the exchange–correlation potential. The equilibrium structural parameters such as lattice constant (a_0), bulk modulus (B_0) and first pressure derivative of bulk modulus (B') are optimized for all alloys. The elastic constants C_{11}, C_{12}, C_{44} and anisotropy coefficients are also estimated. The calculations of the band structure and the density of states demonstrate that all $Be_{1-x}V_xTe$ ($x = 0.25$, 0.50, 0.75 and 1) alloys are complete half-metals. The investigation of the band structure and the density of states demonstrate that $Be_{0.75}V_{0.25}Te$ alloy is entirely half-metal, whereas $Be_{0.50}V_{0.50}Te$ and $Be_{0.25}V_{0.75}Te$ alloys are nearly half-metal. The estimation of the $s(p)$–d exchange splitting constants $N_{0\alpha}$ (conduction band) and $N_{0\beta}$ (valence band), as obtained through the density of states, have been used to indicate the magnetic behavior of the compounds. From the total magnetic moment, it is observed that the p–d hybridization reduces the local magnetic moment of V atom from its free space charge of $3\mu_B$ and generates small local magnetic moments on the nonmagnetic Be and Te sites. Lastly, based on the quasi-harmonic Debye model, the obtained macroscopic thermodynamic properties, such as thermal expansion coefficient, heat capacities and Debye temperate, are presented in detail.

Keywords: Ab-initio calculations; Electronic properties; Magnetic properties; Thermodynamic properties

PACS Nos.: 02.70.-c; 31.15.E-; 61.66.Dk

1. Introduction

The II–VI semiconductors have wide energy band gap and are very attractive materials due to their potential applications in optoelectronics, such as red, blue and green lasers, light-emitting diodes and mid-IR laser sources [1, 2]. Half-metallic ferromagnets (HMFs) and diluted magnetic semiconductors (DMSs) have played a pivotal role in spintronic applications [3], to attain the room temperature ferromagnetism. The HMFs are the most attractive materials due to their particular electronic structure, where one of the two spin channels has a metallic character, whereas the other is semiconducting, leading to 100 % spin-polarization. Also, HMFs have been archived in DMSs or

*Corresponding author, E-mail: murtaza@icp.edu.pk

semimagnetic semiconductors (SMSCs) when a part of nonmagnetic is replaced by magnetic transition metal ions [4]. Since, the first prediction of Groot et al. [5] on the band structures of half-Heusler compounds NiMnSb and PtMnSb, many wide theoretical and experimental applications have been realized in different materials like metal oxides such as Fe_3O_4 [6], CrO_2 [7], full-Heusler compounds Co_2FeSi [8], perovskites alloys $La_{0.7}Sr_{0.3}MnO_3$ [9] and Sr_2FeMoO_6 [10] and in transition metal-doped semiconductors such as, Cr-doped BeSe and BeTe [11, 12], Mn-doped GaN and AlSb [13, 14], $Zn_{1-x}Cr_xS$, $Cd_{1-x}Cr_xS$ and $Cd_{1-x}Cr_xTe$ [15, 16], $Zn_{1-x}Cr_xSe$ [17], $Al_{1-x}Cr_xAs$ [18] and Mn-doped GaAs and V-doped CdTe [19]. Yet there is one experimental realization by doping Cr and Mn in ZnTe up to 1 and 0.2, respectively [20, 21]. This II–VI semiconductor doped with transition metal is a promising compound for room temperature mid-IR lasing [22].

This work is part of a large effort aiming to understand the chemistry–structure–property relationships of the II–VI alloys. In order to do so, a database needs to be created and one of the more intriguing and important questions that this and related work try to answer is: what effects do substitutions on the II or VI sites in the binary II–VI compounds have on properties in general? This understanding allows us to tailor the properties of alloys for any given application. So as first step, it is worth to investigate the evolution of the physical properties of the considered alloy with the concentration of the substituent element from 0 to 100.

The main goal of the present work is the investigation the structural, elastic, electronic, magnetic and thermodynamic properties of zinc blende $Be_{1-x}V_xTe$ alloys for $x = 0.25$, 0.50 and 0.75, using the full-potential linearized augmented plane wave (FP-LAPW) in framework of density functional theory (DFT) within the generalized gradient approximation (GGA) for exchange correlation (EC) functional. It is worthy to note here that: (i) layers are commonly subjected to large built-in strain since they are often grown on different substrates having considerable lattice mismatch within a difference in the thermal expansion coefficients between epitaxial layer and substrate. In the case of the heterostructures and superlattices, this situation becomes more complex and mutual influence between different material layers may appear. This is why, it is necessary to know the elastic constants of the considered materials. (ii) On the other side, theoretical calculations within DFT give material properties at zero temperature only, without any thermal effects included. That is why, it is necessary to calculate the elastic constants and to know the evolution of the physical properties under strain and thermal effects of the considered materials.

2. Calculation method

In this approach, the physical properties of $Be_{1-x}V_xTe$ alloys ($x = 0$, 0.25, 0.50, 0.75 and 1) were estimated using the first-principles FP-LAPW implemented in WIEN2k code [23] within the framework of spin-polarized density functional theory (spin-DFT) [24]. The mechanical properties such as structural and elastic properties were evaluated using GGA of Perdew–Burk–Ernzerhof (PBE) [25], while the electronic and the magnetic properties were estimated employing simultaneously the PBE-GGA and PBE-GGA + U [26], U was chosen as the Hubbard correlation term to describe accurately the correlation effects. The value of Hubbard term U was generally estimated through the comparison between the calculated physical properties and the experimental ones such as band gaps or magnetic moments, if its experimental value was not available. Due to the absence of the experimental values of the physical properties of the studied alloy the value of the of Coulomb repulsion term U of vanadium was taken as 2.73 from [27]. The $R_{MT} \times K_{max}$ parameter was chosen to be 8, with R_{MT} as the smallest muffin-tin radius and K_{max} as the maximum modulus of the reciprocal vector k in the first Brillouin zone. The values of the R_{MT} were taken as 2.22, 2.09 and 2.35 Bohr for Be, Te and V, respectively. The states f Be ($2s^2$), Te ($5s^24d^{10}5p^4$) and V ($4s^23d^3$) were treated as valence electrons. The Brillouin zone integration was performed on $9 \times 9 \times 9$ Monkhorst–Pack scheme with 35 k-point in the first Brillouin zone. The thermodynamic properties of all the alloys were investigated within the quasi-harmonic Debye model implemented in Gibbs program [28]. The self-consistent iterations were converged when the total energy was less than 10^{-4} Ry.

3. Results and discussion

3.1. Structural properties

The structural properties of the binary BeTe and VTe compounds within $Be_{1-x}V_xTe$ ternary alloys ($x = 0.25$, 0.50 and 0.75) in zinc blende (B3) phase have been studied by employing the PBE-GGA parameterization, where the empirical Birch–Murnaghan equation of states [29, 30] is used to minimize the total energy of the system versus unit cell volume and also is served to optimize the equilibrium lattice parameters in ferromagnetic phase such as lattice constant (a_0), bulk modulus (B_0), first derivative of the bulk modulus (B'), and the minimum total energy (E_0), which is given as the following:

$$E(V) = a + bV^{-2/3} + cV^{-4/3} + dV^{-6/3} \quad (1)$$

Here, V is the volume and a, b and c are the fitting parameters. The optimizations of the total energies of compounds versus lattice constant are depicted in Fig. 1(a)–1(d).

Table 1 shows the obtained values of the equilibrium lattice constant (a_0), bulk modulus (B_0) and first derivative of the bulk modulus (B'), which are compared with those of other available works. There is a very good agreement between the calculated value of the lattice parameter of BeTe and the available experimental data [31]; the deviation is less than +0.5 %, which indicates the reliability of the present results. One can also note the reasonable agreement between the calculated lattice parameters for the parent compounds, BeTe and VTe and those performed by previous calculations [32–36]. The maximum deviation does not exceed 2.94 %. Deviations between our calculated values for the bulk moduli of the parent compounds, BeTe and VTe and those available in the literature are about 12.31 and 19.49 %, respectively, which would be attributed to the technical difficulty to measure the bulk modulus and on another side to the sensibility of the bulk modus value to the used method to treat the exchange–correlation potential. It is worth to note that there are no experimental or theoretical data for the ternary $Be_{1-x}V_xTe$ alloys for $x = 0.25$, 0.50 and 0.75, for comparison. The evaluation of the lattice constant and bulk modulus of the $Be_{1-x}V_xTe$ alloys as a function of V concentration is illustrated in Fig. 2(a) and 2(b). One can easily observe that the lattice constant decreases, while the bulk modulus increases with increasing x. The augmentation of the doping chemical element V concentration reinforces the hardness of the alloys.

3.2. Elastic properties

The elastic moduli of the $Be_{1-x}V_xTe$ alloys in zinc blende structure have been calculated using the method elaborated by Thomas Charpin and implemented in Wien2k package [23]. In general, the elastic moduli are obtained from the general Hook's law that relates stresses (σ) with the corresponding strains (ε) as follows:

$$\begin{bmatrix} \sigma 11 \\ \vdots \\ \sigma 61 \end{bmatrix} = \begin{bmatrix} C11 & \cdots & C16 \\ \vdots & \ddots & \vdots \\ C61 & \cdots & C66 \end{bmatrix} \times \begin{bmatrix} \varepsilon 11 \\ \vdots \\ \varepsilon 61 \end{bmatrix} \quad (2)$$

The elastic constants are C_{11}, C_{12} and C_{44}, when three equations are needed to determine these elastic constants. The first equation is the formula of the bulk modulus.

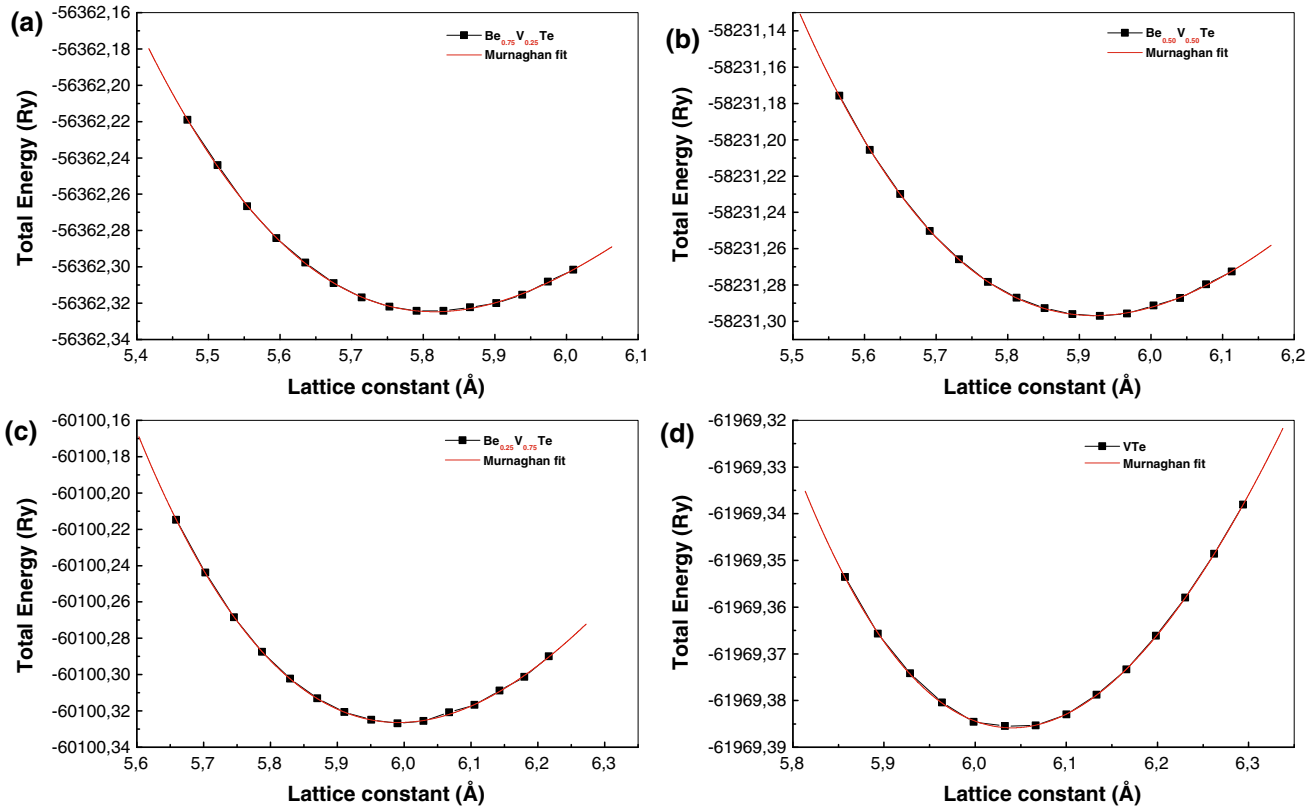

Fig. 1 Variation of calculated total energy with lattice for ZB $Be_{1-x}V_xTe$ alloys at (**a**) $x = 0.25$, (**b**) $x = 0.50$, (**c**) $x = 0.75$ and (**d**) $x = 1$. The *solid lines* through data are fits to the Murnaghan equation of states

Table 1 The calculated equilibrium lattice constant a_0, bulk modulus B and its pressure derivative B' for ZB $Be_{1-x}V_xTe$ using the BPE-GGA and PBE-GGA + U approximations

Composition	Lattice parameter a_0 (Å)			Bulk modulus B (GPa)			B'		
X	This work	Cal	Exp	This work	Cal	Exp	This work	Cal	Exp
0.00	5.645	5.671[b]	5.617[a]	60.33	56.128[b]	68.8[a]	4.16	6.21[b]	–
		5.531[c]			70.0[c]			3.38[c]	–
0.25	5.818	–	–	59.53	–	–	4.15	–	–
0.50	5.923	–	–	62.19	–	–	4.32	–	–
0.75	5.993	–	–	66.18	–	–	4.39	–	–
1.00	6.040	6.223[d]	–	68.90	57.66[f]	–	4.60	50.3[d]	–
		6.271[e]							

[a] Ref. [31]; [b] Ref. [32]; [c] Ref. [33]; [d] Ref. [34]; [e] Ref. [35]; [f] Ref. [36]

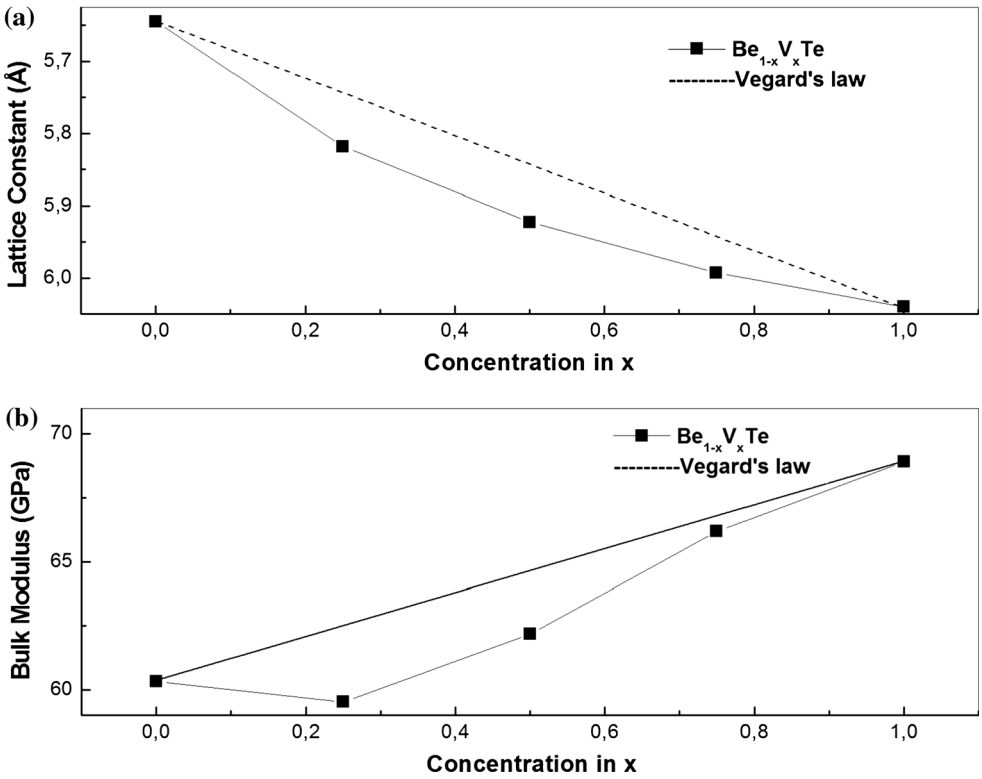

Fig. 2 Comparison between the calculated (**a**) lattice constant and (**b**) bulk modulus for ZB $Be_{1-x}V_xTe$ alloys on the values obtained from Vegard's law for different contours

$$B = (C_{11} + 2C_{12})/3 \tag{3}$$

The second one involves the volume-conserving tetragonal strain tensor.

$$\begin{bmatrix} \delta & 0 & 0 \\ 0 & \delta & 0 \\ 0 & 0 & \frac{1}{(1+\delta)^2} - 1 \end{bmatrix} \tag{4}$$

Application of this strain changes the total energy from its unstrained value as follows:

$$E(\delta) = E(0) + 6(C_{11} - C_{12})V_0\delta^2 + O(\delta^3) \tag{5}$$

where V_0 is the unit cell volume and $O(\delta^3)$ term represents the errors of the adjustment.

The third one involves the volume-conserving rhombohedral strain tensor, which determines the C_{44} modulus.

$$\frac{\delta}{3}\begin{bmatrix} 1 & 1 & 1 \\ 1 & 1 & 1 \\ 1 & 1 & 1 \end{bmatrix} \tag{6}$$

The total energy is changed to become

$$E(\delta) = E(0) + (C_{11} + 2C_{12} + 4C_{44})V_0\delta^2 + O(\delta^3) \quad (7)$$

The mechanical stability of the cubic crystal must satisfy the Born stability criteria [37].

$$C_{44} > 0 \quad (8)$$

$$C_{11} - |C_{12}| > 0 \quad (9)$$

$$C_{11} + 2C_{12} > 0 \quad (10)$$

The obtained values of elastic constants; C_{11}, C_{12} and C_{44} are given in Table 2 along with other results available in the literature for comparison. No reported results are available for the elastic moduli of the ternary alloys $Be_{1-x}V_xTe$, where $x = 0.25$, 0.50 and 0.75. There is a good agreement between our calculated values for C_{11}, C_{12} and C_{44} of BeTe and the previously calculated one [38–41]. All calculated elastic constants for all alloys, i.e. $x = 0$–1, satisfy the well-known Born stability criteria. Thus, all the $Be_{1-x}V_xTe$ alloys are mechanically stable.

The elastic anisotropy has a great importance for many mechanical-physical properties such as unusual phonon modes, phase transformations, precipitation, dislocation dynamics, anisotropic plastic deformation, crack behavior, elastic instability, internal friction [42]. Moreover, recent research [43] demonstrates that the elastic anisotropy has a significant influence on the nanoscale precursor textures in alloys. Therefore, several criteria have been developed to investigate the elastic nature of materials. In the present case, two different approaches have been used to represent the elastic anisotropy of the $Be_{1-x}V_xTe$ alloys in zinc blende structure: The elastic anisotropy factor, which is defined as $A = 2C_{44}$–$(C_{11}$–$C_{12})/C_{11}$ [44–48] and the universal elastic anisotropy factor developed by Ranganathan and Ostoja–Starzewski [45], $A^U = 6/5 \times \left(\sqrt{A'} - 1/\sqrt{A'}\right)^2$, where A' is Ziner anisotropy ratio, which is defined as $A' = 2C_{44}/(C_{11}-C_{12})$ [44]. Here, $A^U = 0$ for isotropic crystals and deviation from zero reflects the degree of single-crystal elastic anisotropy. Table 3 collects the obtained values of A and A^U, which reveals that the considered alloys exhibit a noticeable degree of elastic anisotropy.

3.3. Electronic properties

The spin-polarized band structure energies of zinc blende $Be_{1-x}V_xTe$ alloys ($x = 0.25$, 0.50 and 0.75) are evaluated at their equilibrium lattice parameter using the two PBE-GGA and PBE-GGA + U schemes. These predictions are served to precise the potential used in spintronic and optoelectronics. The obtained values of the band gap of minority-spin (E_g) and the half-metallic gap (E_{HM}) are given in Table 4. It is noted that the values of E_{HM} obtained with PBE-GGA + U are improved than those obtained with PBE-GGA, the electronic band structures of $Be_{1-x}V_xTe$ at $x = 0.25$, 0.50 and 0.75 are shown in Figs. 3(a)–3(d), 4(a)–4(d), 5(a)–5(d), respectively, along the high symmetry direction in the first Brillouin zone by employing the both PBE-GGA and PBE-GGA + U schemes, where bottom of the conduction band and top of the valence band are at symmetry point Γ. The predictions obtained with PBE-GGA approximation exhibit the energy bands in majority-spin states (spin-up) cross the Fermi level, while in minority-spin states (spin-down), the energy bands are situated under the Fermi level confirming the half-metallic property. For $Be_{0.50}V_{0.50}Te$ and $Be_{0.25}V_{0.75}Te$ alloys, one energy band cut the Fermi level at point Γ, so $Be_{0.75}V_{0.25}Te$ alloy exhibits half-metallic character, whereas $Be_{0.50}V_{0.50}Te$ and $Be_{0.25}V_{0.75}Te$ alloys are nearly half-metal. The electronic results obtained using PBE-GGA + U scheme depict all the $Be_{1-x}V_xTe$ alloys ($x = 0.25$, 0.50 and 0.75) are half-metal with E_{HM} values for each corresponding concentration. The half-metallic energy gap (E_{HM}) is defined as the maximum between the lowest energy of majority-spin and the minority-spin conduction bands with respect to the Fermi level and the

Table 2 Elastic constant (in GPa) for ZB $Be_{1-x}V_xTe$ using the BPE-GGA approximation

Composition	C_{11}			C_{12}			C_{44}		
X	This work	Cal	Exp	This work	Cal	Exp	This work	Cal	Exp
0.00	109.91	111.7[a]	–	35.49	35.5[a]	–	62.25	63.7[a]	–
		104[b]			35[b]			59[b]	
		85.56[c]			59.94[c]			13.6[c]	
		99[d]			44[d]			68[d]	
0.25	93.29	–	–	42.59	–	–	60.76	–	–
0.50	82.49	–	–	51.98	–	–	58.41	–	–
0.75	71.78	–	–	63.28	–	–	57.87	–	–
1.00	67.07	–	–	75.06	–	–	56.64	–	–

[a] Ref. [38]; [b] Ref. [39]; [c] Ref. [40]; [d] Ref. [41]

Table 3 Calculating anisotropy (A), Ziner anisotropy ratio (A') and universal anisotropy (A^U) for ZB $Be_{1-x}V_xTe$ using the BPE-GGA approximation

Composition	A			A'			A^U		
X	This work	Cal	Exp	This work	Cal	Exp	This work	Cal	Exp
0.00	0.4555	–	–	1.6729	–	–	0.3248	–	–
0.25	0.7591	–	–	2.3968	–	–	0.9768	–	–
0.50	1.0463	–	–	3.8289	–	–	2.5081	–	–
0.75	1.4940	–	–	13.6165	–	–	14.028	–	–
1.00	1.8081	–	–	−14.177	–	–	–	–	–

Table 4 The calculated results of the half-metallic E_{HM} (eV) band gaps and spin-minority band gaps E_g (eV) of each site in $Be_{1-x}V_xTe$ alloys obtained using the PBE-GGA and PBE-GGA + U schemes

Alloy	Composition	E_g			E_{HM}		
	X	This work	Cal	Exp	This work	Cal	Exp
BeTe	0.00	1.77 (1.77)	1.72[a]	2.70[f]			
			1.81[b]				
			1.90[c]				
$Be_{0.75}V_{0.25}Te$	0.25	2.18 (2.45)	2.60[d]	–	0.18 (0.55)	–	–
$Be_{0.50}V_{0.50}Te$	0.50	1.96 (2.15)	2.67[d]	–	– (0.42)	–	–
$Be_{0.25}V_{0.75}Te$	0.75	2.28 (2.34)	2.69[d]	–	– (0.02)	–	–
Vte	1.00	2.74 (2.45)	2.95[d]	–	– (0.03)	0.05[e]	–
			2.80[e]				

[a] Ref. [39]; [b] Ref. [40]; [c] Ref. [41]; [d] Ref. [46]; [e] Ref. [36]; [f] Ref. [47]

absolute values of the highest energy of majority-spin and minority-spin valence bands [48, 49]. The obtained values of E_{HM} decrease with increasing concentration of V-doped atom for $x = 0.25$–0.75. The obtained values of E_{HM} by GGA + U, lead to archiving high Curie temperature in $Be_{1-x}V_xTe$ alloys [50]. Through the obtained results in electronic structure, the PBE-GGA + U parameterization reveals excellence predictions, due to fact of U-Hubbard correlation, which is fully influenced the V-$3d$ states.

The electronic density of states (DOS) is to investigate the electronic structure in detail. The total and partial densities of states (TDOS and PDOS) of $Be_{1-x}V_xTe$ alloys in ferromagnetism phase are estimated at their equilibrium lattice parameters and plotted in Figs. 6(a)–6(f) and 7(a)–7(f).

About the Fermi level, there is a large exchange splitting between spin-up and spin-down states. From the TDOS of all $Be_{1-x}V_xTe$ ($x = 0.25$, 0.50 and 0.75) alloys calculated using PBE-GGA, it is noted that the alloys show the metallic character due to spin-up electrons, while for spin-down electrons, the alloys have semiconducting behavior, through confirming the half-metallic nature of these alloys. The $Be_{0.50}V_{0.50}Te$ and $Be_{0.25}V_{0.75}Te$ alloys are nearly half-metal, which is due to one energy band cross the Fermi level. From the obtained results of PBE-GGA + U scheme, all the three compounds confirm the half-metallic characteristic. In the PDOS versus energy curves for all alloys through PBE-GGA and PBE-GGA + U, the states between −11.5 and −13 eV mainly originate from Be s states. The bands in energy range from −6.65 to −1.99 eV of PBE-GGA approach and form −6.42 to −1.73 eV of GGA + U approach mainly originate from Te-5p with some contributions of V-3d and Be-2s states. Therefore, around the Fermi level, the top part of the valence band and bottom part of conduction band arise from V-3d states, where there is a strong hybridization between V-3d and Te-5p states, which is responsible for the half-metallic property. The V-3d states are divided into V − t_{2g} and V-e.g., where in the region around the Fermi level, it exists an intense V t_{2g}-Te 5p hybridization and a weak V e.g.-Te 5p hybridization.

For the V atom, the V-3d states band exchange splitting $\Delta_x(d)$, defined as a difference between majority-spin and minority-spin peaks, are estimated and listed in Table 5. An important parameter to describe the nature of attraction is the p–d exchange splitting $\Delta_x(pd)$, which is defined as:

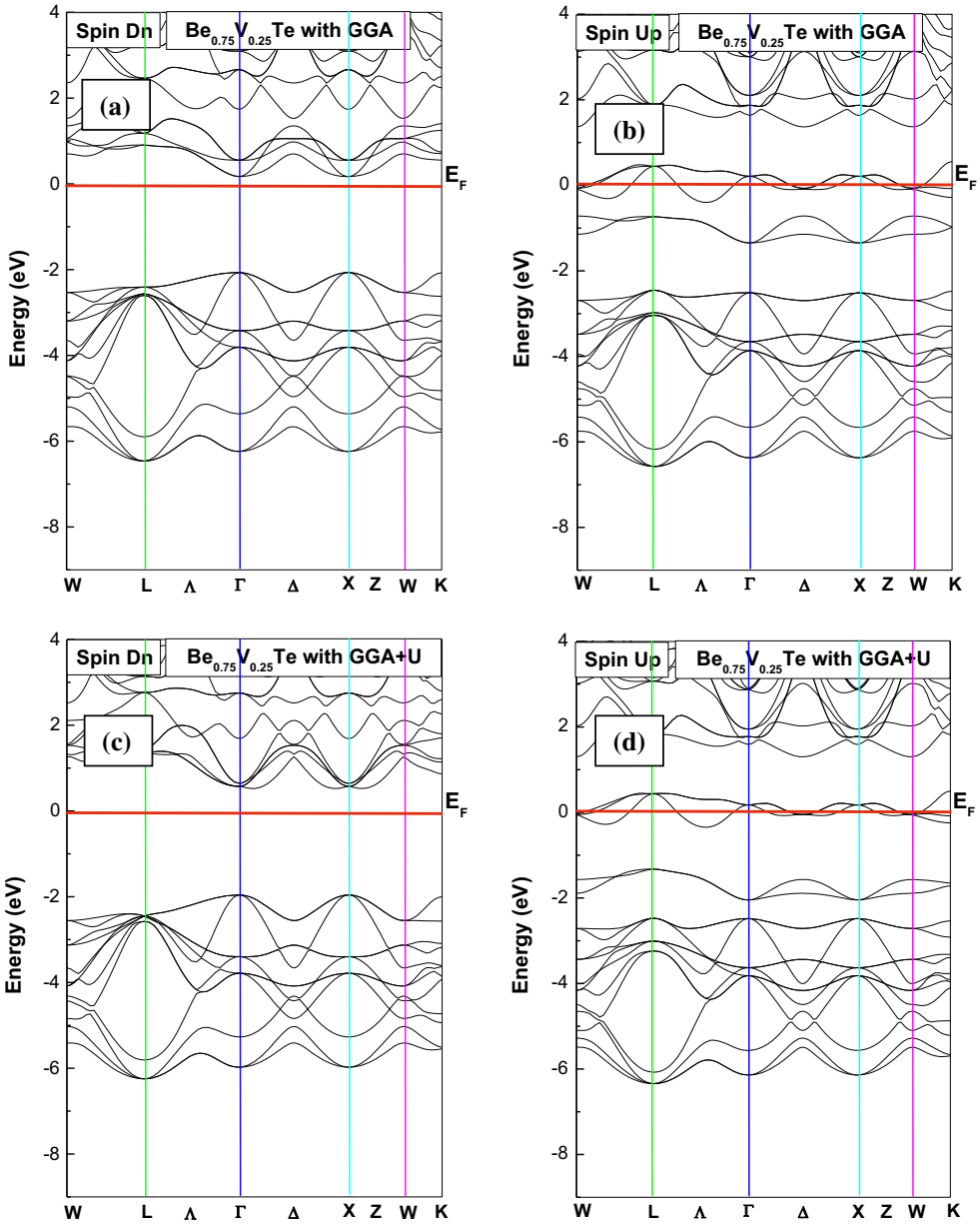

Fig. 3 Spin-polarized electronic band structures of $Be_{0.75}V_{0.25}Te$ alloys at the equilibrium lattice parameter obtained using GGA and GG A + U schemes: (**a**) GGA spin down, (**b**) GGA spin up, (**c**) GGA + U spin down and (**d**) GGA + U spin up

$$\Delta_x(pd) = E_v(\downarrow) - E_v(\uparrow) \tag{11}$$

where $E_v(\downarrow)$ and $E_v(\uparrow)$ are the valence band maxima of spin-down and spin-up, respectively. The negative sign of the obtained values of $\Delta_x(pd)$ reveals that the effective potential is more attractive for spin-down case in comparison with spin-up case [51].

3.4. Magnetic properties

The study of the electronic structure in detail is useful to determine two important parameters of exchange splitting, namely the s–d exchange constant $N_0\alpha$ (conduction band) and p–d exchange constant $N_0\beta$ (valence band), where N_0 signifies the concentration of the cations. These parameters are served to evaluate the comparison between valence and conduction bands affected during the exchange splitting process. Through the Kondo interactions, the exchange constants can be determined as [52]:

$$N_o\alpha = \frac{\Delta E_c}{x(S)}; \quad N_o\beta = \frac{\Delta E_v}{x(S)} \tag{12}$$

where ΔE_c and ΔE_v are the respective conduction and valence edge splitting, x is the concentration of V atom and $\langle S \rangle$ is one-half magnetization of V atom. The obtained values of $N_0\alpha$ and $N_0\beta$ are given in Table 5. We observe that the obtained results of $N_0\alpha$ and $N_0\beta$ from the GGA + U calculations are in opposite sign and

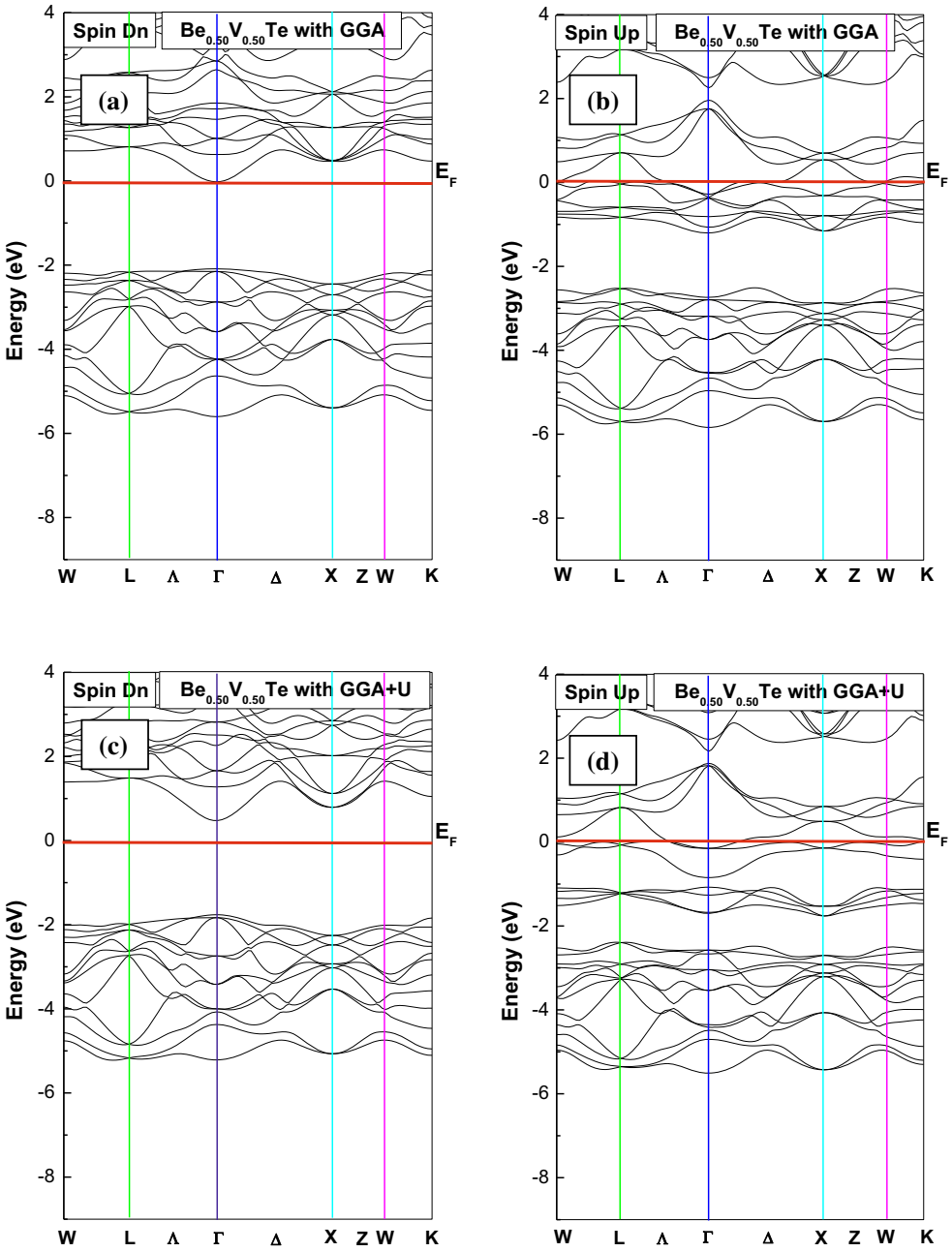

Fig. 4 Spin-polarized electronic band structures of $Be_{0.50}V_{0.50}Te$ alloys at the equilibrium lattice parameter obtained using GGA and GGA + U schemes: (**a**) GGA spin down, (**b**) GGA spin up, (**c**) GGA + U spin down and (**d**) GGA + U spin up

consequently confirm that the valence and conduction bands have an opposite behavior during the exchange splitting process. Moreover, the values of exchange constants decrease with the increasing concentration of V in the range from 0.25 to 1, where the V-*3d* states dominate over the Te-*5p* states and also these results confirms the magnetic nature of the alloys.

The total magnetic moment (M_{Tot}) of $Be_{1-x}V_xTe$ alloys ($x = 0.25$, 0.50, 0.75 and 1) and the local magnetic moments of Be, V and Te atoms, obtained using both PBE-GGA and PBE-GGA + U methods are shown in Table 6. Obviously, the change of the total magnetic moment follows Hund's rule. We observe that the obtained results of the total magnetic moment is mainly arise from transition metal of V-doped atom with small contributions comes from Be and Te sites. The atomic magnetic moment of V is reduced from its free space charge of $3\mu_{\mathrm{B}}$ and small local magnetic moments are produced on the nonmagnetic Be and Te sites, arising from the strong p–d hybridization between V-t_{2g} states and Te-*5p* states. Furthermore, the

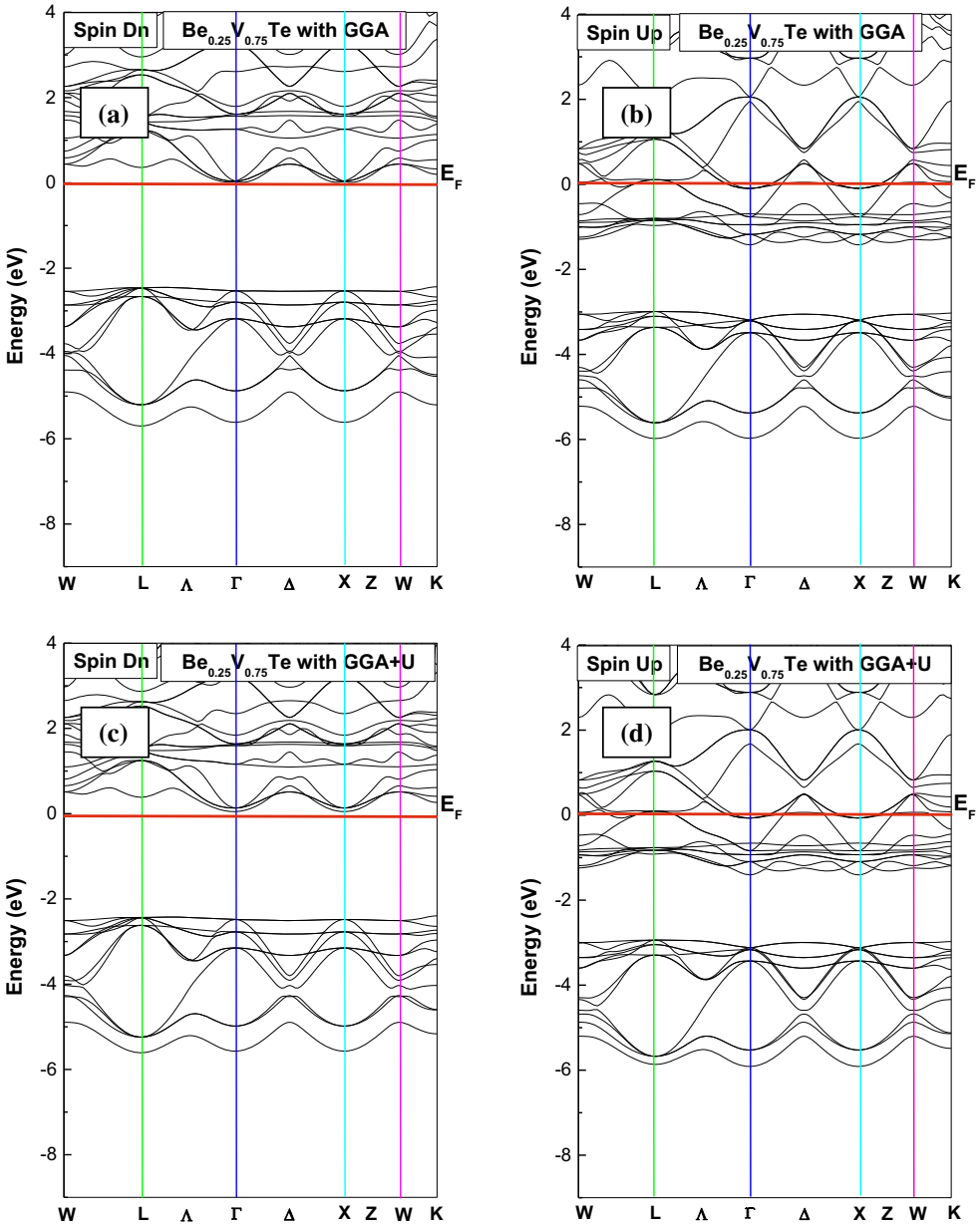

Fig. 5 Spin-polarized electronic band structures of $Be_{0.25}V_{0.75}Te$ alloys at the equilibrium lattice parameter obtained using GGA and GGA + U schemes: (**a**) GGA spin down, (**b**) GGA spin up, (**c**) GGA + U spin down and (**d**) GGA + U spin up

values of the local magnetic moment of V and Te atoms have opposite signs, indicating that valence band containing Te-*5p* and V-*3d* spins interacts antiferromagnetically.

3.5. Thermodynamic properties

The thermodynamic properties of the zinc blende $Be_{1-x}V_xTe$ alloys ($x = 0.25$, 0.50 and 0.75) are investigated under high temperature based on the quasi-harmonic Debye model, implemented in Gibbs program [28] to study the macroscopic properties, such as thermal expansion coefficient (α), heat capacity at constant volume (C_v) and Debye temperature (θ_D). These parameters have been plotted in Fig. 8(a)–8(c), respectively, as a function of temperature.

In the first step, Fig. 8(a) depicts that α increases for the three alloys, where in case of $Be_{0.75}V_{0.25}Te$ and $Be_{0.50}V_{0.50}Te$ alloys, it increases brutally in the range from 0 to 100 K. Above 100 K, its increases slowly to a constant value. The thermal expansion coefficient of the $Be_{0.75}V_{0.25}Te$, $Be_{0.50}V_{0.50}Te$ and $Be_{0.25}V_{0.75}Te$ alloys at room temperature and zero pressure are 0.509×10^5, 1.12×10^5 and 0.04×10^5 K^{-1}, respectively.

It is given in Fig. 8(b) that at low temperature the C_v for the three compounds is proportional to T^3 [53], whereas at high temperatures, C_v for all the alloys converges to Petit and Dulong limit [54]. The obtained C_v values of $Be_{0.75}V_{0.25}Te$, $Be_{0.50}V_{0.50}Te$, $Be_{0.25}V_{0.75}Te$ alloys are 70.33, 70.90 and 70.35 J mol^{-1} K^{-1}, respectively.

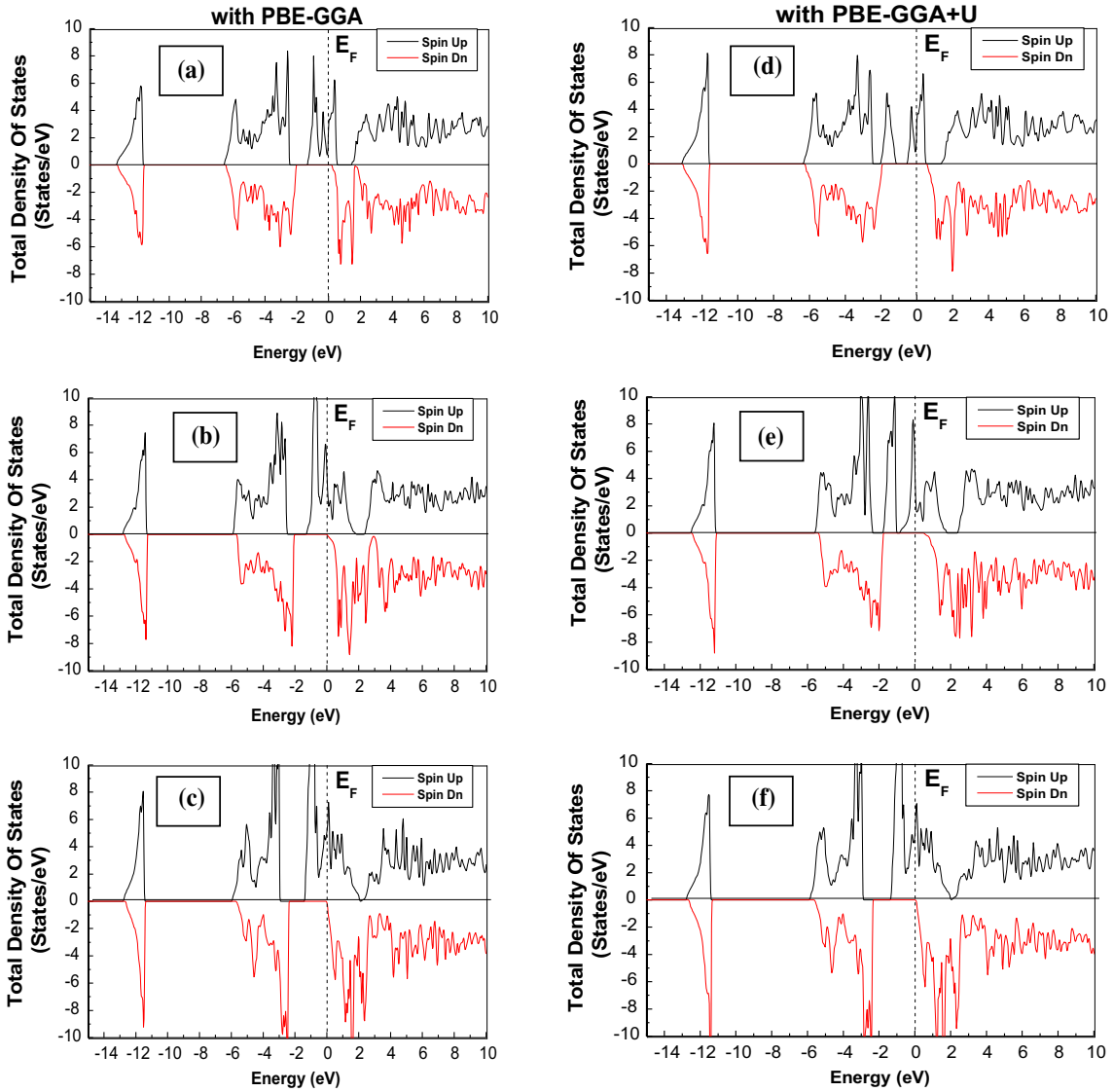

Fig. 6 Spin-dependent total density of states; (**a**) $Be_{0.75}V_{0.25}Te$, (**b**) $Be_{0.50}V_{0.50}Te$, (**c**) $Be_{0.25}V_{0.75}Te$ using GGA and (**d**) $Be_{0.75}V_{0.25}Te$, (**e**) $Be_{0.50}V_{0.50}Te$, (**f**) $Be_{0.25}V_{0.75}Te$ obtained using GGA + U

It is noticed in Fig. 8(c) that for $Be_{0.75}V_{0.25}Te$ and $Be_{0.50}V_{0.50}Te$ alloys, θ_D is nearly constant in the range from 0 to 100 K and decrease slowly, whereas it is absolutely constant in case of $Be_{0.25}V_{0.75}Te$ alloy. At the room temperature and zero pressure, the θ_D of $Be_{0.75}V_{0.25}Te$, $Be_{0.50}V_{0.50}Te$ and $Be_{0.25}V_{0.75}Te$ alloys are 336.30, 313.38 and 335.53 K, respectively.

4. Conclusions

We have studied the structural, elastic, electronic, magnetic and thermodynamic properties of zinc blende $Be_{1-x}V_xTe$ alloys ($x = 0$, 0.25, 0.50, 0.75 and 1) using the first-principles FP-LAPW method within the DFT theory. The results of spin-polarized GGA + U calculation demonstrate that all $Be_{1-x}V_xTe$ alloys ($x = 0.25$, 0.50, 0.75 and 1) are totally half-metal ferromagnetic materials. In comparison, the PBE-GGA + U scheme provides improved results than that of the PBE-GGA scheme. The three $Be_{1-x}V_xTe$ alloys ($x = 0.25$, 0.50 and 0.75) are elastically stable. From the total density of states and partial density of states curves, the exchange splitting $\Delta_x(d)$ and $\Delta_x(pd)$ parameters are estimated to describe the exchange splitting process due to V-*3d* effect. The negative sign of $\Delta_x(pd)$ proves that the effective potential is more attractive for spin-down case than spin-up case. Our values of the exchange constants $N_0\alpha$ and $N_0\beta$ are in opposite signs, indicating that the valence and the conduction spins interact oppositely during the exchange splitting process. In fact,

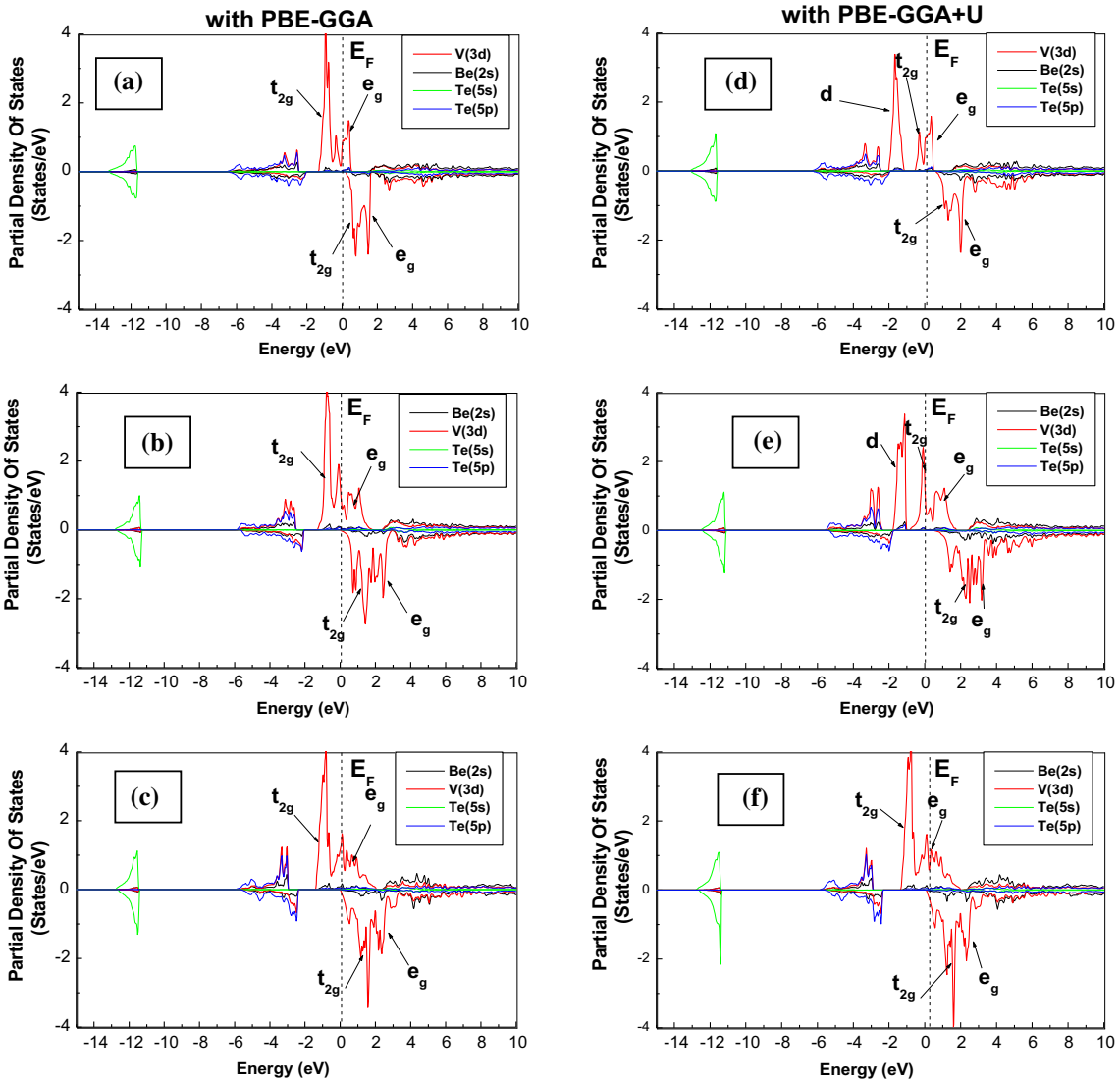

Fig. 7 Spin-dependent partial density of states; (**a**) $Be_{0.75}V_{0.25}Te$, (**b**) $Be_{0.50}V_{0.50}Te$, (**c**) $Be_{0.25}V_{0.75}Te$ using GGA and (**d**) $Be_{0.75}V_{0.25}Te$, (**e**) $Be_{0.50}V_{0.50}Te$, (**f**) $Be_{0.25}V_{0.75}Te$ obtained using GGA + U

Table 5 The calculated conduction and valance band-edge spin-splitting $\Delta_x(d)$, $\Delta_x(pd)$ and exchange constants of $Be_{1-x}V_xTe$ for (a) $x = 0.25$, (b) $x = 0.50$ and (c) $x = 0.75$, using PBE-GGA and PBE-GGA + U schemes

Alloy	x	$\Delta_x(d)$	$\Delta_x(pd)$	$N_0\alpha$	$N_0\beta$
$Be_{1-x}V_xTe$	0.25	2.422 (0.952)	−1.999 (−1.903)	0.355 (1.092)	−3.998 (−3.806)
	0.50	2.204 (1.224)	−2.024 (−1.728)	−0.065 (0.421)	−2.024 (−1.728)
	0.75	2.422 (0.707)	−2.342 (−2.323)	−0.037 (0.011)	−1.561 (−1.549)

Table 6 The calculated results of the total magnetic moment (M_{tot} in μ_B) per V atom and local magnetic moment of each concentration for ZB $Be_{1-x}V_xTe$ obtained using PBE-GGA and PBE-GGA + U schemes

Alloy	$Be_{0.75}V_{0.25}Te$	$Be_{0.50}V_{0.50}Te$	$Be_{.25}V_{0.75}Te$	VTe
M_{Tot}	3.001 (2.995)	2.999 (3.001)	3.009 (3.000)	2.544 (2.950)
M_V	2.253 (2.494)	2.377 (2.583)	2.494 (2.508)	2.254 (2.659)
M_{Be}	0.062 (0.057)	0.105 (0.079)	0.142 (0.134)	–
M_{Te}	−0.019 (−0.038)	−0.033 (−0.055)	−0.052 (−0.057)	−0.063 (−0.102)

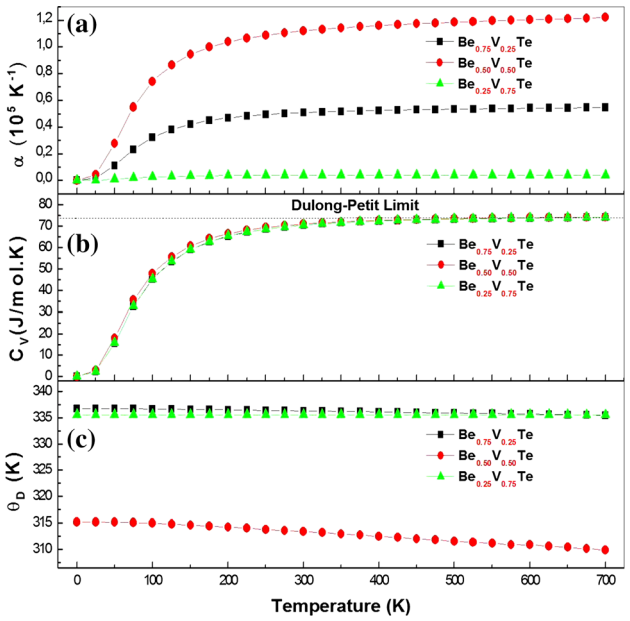

Fig. 8 Variation of (**a**) thermal expansion α, (**b**) heat capacity *Cv* and (**c**) Debye temperature θ_D with temperature at zero pressure for ZB $Be_{1-x}V_xTe$ alloys ($x = 0.25$, 0.50 and 0.75)

the *p–d* hybridization between V-t_{2g} and Te-*5p* states reduces the atomic magnetic moment of V from its free space charge of $3\mu_B$ its also appears small local magnetic moments at the nonmagnetic Be and Te atoms. Moreover, the local magnetic moment of V atom contributes mainly to the total magnetic moment of the compounds. Based on the quasi-harmonic Debye model implemented in Gibbs program, the thermal expansion coefficient (α), specific heat capacity at constant volume (C_v) and Debye temperature (θ_D) versus temperature are investigated.

Acknowledgments R Khenata, A Bouhemadou and S Bin Omran acknowledge the financial support provided by the Deanship of Scientific Research at King Saud University through the research group Project No. RPG-VPP-088.

References

[1] M C Tamargo, A Cavus, L Zeng, N Dai, N Bambha and A Gray *J. Elecron. Mater.* **25** 259 (1996)
[2] O Maksimov, S P Guo and M C Tamargo *Appl. Phys. Lett.* **78** 2473 (2001)
[3] K Y Ko and M G Blamire *J. Korean Phys. Soc.* **49** 591 (2006)
[4] W Mac et al. *Phys. B* **211** 384 (1995)
[5] R A de Groot, F M Mueller, P G van Engen and K H J Buschow *Phys. Rev. Lett.* **50** 2024 (1983)
[6] F J Jedema, A T Filip and B V Wees *Nature* **410** 345 (2001)
[7] K Schwarz *J. Phys. F Met. Phys.* **16** L211 (1986)
[8] S Wurmehl, G H Fecher, H C Kandpal, V Ksenofontov, C Felser and H J Lin *Appl. Phys. Lett.* **88** 032503 (2006)
[9] R J Soulen Jr et al. *Science* **282** 85 (1998)
[10] K L Kobayashi, T Kimura, H Sawada, K Terakura and Y Tokura *Nature* **395** 677 (1998)
[11] S Picozzi, T Shishidou, A J Freeman and B Delly *Phys. Rev. B* **67** 165203 (2003)
[12] S M Alay-e-Abbas, K M Wong, N A Noor, A Shaukat and Y Lei *Solid State Sci.* **14** 1525 (2012)
[13] T Jungwirth, J Sinova, J Mašek, J Kučera and A H Mac Donald *Rev. Mod. Phys.* **78** 809 (2006)
[14] G Rahman, S Cho and S C Hong *Phys. Status Solidi B* **12** 4435 (2007)
[15] [15] S Nazir, N Ikram, S A Siddiqi, Y Saeed, A Shaukat and A H Reshak *Curr. Opin. Solid State Mater. Sci.* **14** 1 (2010)
[16] N A Noor, S Ali and A Shaukat *J. Phys. Chem. Solids* **72** 836 (2011)
[17] X-F Ge and Y-M Zhang *J. Magn. Magn. Mater.* **321** 198 (2009)
[18] Y-H Zhao and G-P Zhao *Phys. Rev. B* **80** 224417 (2009)
[19] G Y Gao, K L Yao, Z L Liu, Y L Li, J L Jiang and Y C Li *Phys. B* **382** 14 (2006)
[20] T M Giebultowicz, P Klosowski, N Samarth and J K Furdyna *Phys. Rev. B* **48** 12817 (1993)
[21] H Saito, V Zayets, S Yamagata and K Ando *Phys. Rev. Lett.* **90** 207202 (2003)
[22] S Mirov, V Fedorov, I Moskalev, D Martyshkin and C Kim *Laser Photon. Rev.* **4** 21 (2009)
[23] P Blaha, K Schwarz, P Sorantin and S K Trickey *Comput. Phys. Commun.* **59** 339 (1990)
[24] P Hohenberg and W Kohn *Phys. Rev.* **136** B864 (1964)
[25] J P Perdew, S Burke and M Ernzerhof *Phys. Rev. Lett.* **77** 3865 (1996)
[26] V I Anisimov, I V Solovyev, M A Korotin, M T Czyzyk and G A Sawatzky *Phys. Rev. B* **48** 16929 (1993)
[27] J Kaczkowski and A Jezierski *Acta Phys. Pol. A* **105** 924 (2009)
[28] M A Blanco, E Francisco and V Luaña *Comput. Phys. Commun.* **158** 57 (2004)
[29] F D Murnaghan *Proc. Natl. Acad. Sci. USA* **30** 5390 (1944)
[30] S L Shang, Y Wang, D Kim and Z-K Liu *Comput. Mater. Sci.* **47** 1040 (2010)
[31] H Luo, K Ghandehari, R G Greene, A L Ruoff, S S Trail and F J Disalvo *Phys. Rev. B* **52** 7058 (1995).
[32] H Baaziz, Z Charifi, F El Haj Hassan, S J Hashemifar and H Akbarzadeh *Phys. Status Solidi B* **243** 1296 (2006)
[33] M González-Diáz, P Rodríguez-Hermández and A Munoz *Phys. Rev. B* **55** 14043 (1997)
[34] D Huang, Y J Zhao, L J Chen, D H Chen and Y Z Shao *J. Appl. Phys.* **104** 053709 (2004)
[35] W-H Xie, Y-Q Xu, B-G Liu and D G Pettifor *Phys. Rev. Lett.* **91** 037204 (2003)
[36] M Sajjad, H X Zhang, N A Noor, S M Alay-e-Abbas, A Shaukat and Q Mahmood *J. Magn. Magn. Mater.* **343** 177 (2013)
[37] J F Nye *Physical Properties of Crystals: Their Representation by Tensors and Matrices* (Oxford, UK: Oxford University Press) (1985)
[38] F El Haj Hassan and H Akbarzadeh *Comp. Mater. Sci.* **35** 423 (2006)
[39] D Heciri et al. *Comp. Mater. Sci.* **38** 609 (2007)
[40] D Rached et al. *Comput. Mater. Sci.* **37** 292 (2006)
[41] R Khenata, A Bouhemadou, M Hichour, H Baltache, D Rached and M Rérat *Solid State Electron.* **50** 1382 (2006)
[42] H Ledbetter, A Migliori *J. Appl. Phys.* **100** 063516 (2006)
[43] P Lloveras, T Castán, M Porta, A Planes and A Saxena *Phys. Rev. Lett.* **100** 165707 (2008)
[44] B B Karki, L Stixture, S J Clark, M C Warren and G G Ackland *J. Grain Am. Miner.* **82** 51 (1997)
[45] S I Ranganathan and M Ostoja-Starzewski *Phys. Rev. Lett.* **101** 055504 (2008)
[46] M Sajjad et al. *J. Magn. Magn. Mater.* **379** 63 (2015)
[47] W M Yim, J B Dismakes, E J Stofko and R J Paff *J. Phys. Chem. Solids* **33** 501(1972)

[48] K L Yao, G Y Gao, Z L Liu and L Zhu *Solid State Commun.* **133** 301 (2005)
[49] G Y Gao, K L Yao, E Sasioglu, L M Sandratskii, Z L Liu and J L Jiang *Phys. Rev. B* **75** 174442 (2007)
[50] J Kubler *Phys. Rev. B* **67** 220403R (2003)
[51] V L Morozzi, J F Janak and A R Williams *Calculated Electronic Properties of Metals* (NewYork: Pergamon) (1978)
[52] J A Gaj, R Planel and G Fishman *Solid State Commun.* **29** 861 (1984)
[53] P Debye *Ann. Phys.* **39** 789 (1912)
[54] A T Petit and P L Dulong *Ann. Chim. Phys.* **10** 395 (1819)